Published December 1, 1986

Fluorescence Visualization of the Distribution of Microfilaments in Gonads and Early Embryos of the Nematode *Caenorhabditis elegans*

Susan Strome

Department of Biology, Indiana University, Bloomington, Indiana 47405

Abstract. Several intracellular motility events in the *Caenorhabditis elegans* zygote (pseudocleavage, the asymmetric meeting of the pronuclei, the segregation of germ line–specific granules, and the generation of an asymmetric spindle) appear to depend on microfilaments (MFs). To investigate how MFs participate in these manifestations of zygotic asymmetry, the distribution of MFs in oocytes and early embryos was examined, using both antibodies to actin and the F-actin–specific probe rhodamine–phalloidin. In early-stage zygotes, MFs are found in a uniform cortical meshwork of fine fibers and dots or foci. In later zygotes, concomitant with the intracellular movements that are thought to be MF mediated, MFs also become asymmetrically rearranged; as the zygote undergoes pseudocleavage and as the germ line granules become localized in the posterior half of the cell, the foci of actin become progressively more concentrated in the anterior hemisphere. The foci remain anterior as the spindle becomes asymmetric and the zygote undergoes its first mitosis, at which time fibers align circumferentially around the zygote where the cleavage furrow will form. A model for how the anterior foci of actin may participate in zygotic motility events is discussed.

Phalloidin and anti–actin antibodies have also been used to visualize MFs in the somatic tissues of the adult gonad. The myoepithelial cells that surround maturing oocytes are visibly contractile and contain an unusual array of MF bundles; the MFs run roughly longitudinally from the loop of the gonad to the spermatheca. Myosin thick filaments are distributed along the MFs in a periodic manner suggestive of a sarcomere-like configuration. It is proposed that these actin and myosin filaments interact to cause sheath cell contraction and the movement of oocytes through the gonad.

A critical aspect of early embryonic development is the generation of asymmetry and production of different cell types. In all organisms, the fertilized egg must give rise to blastomeres that differ in developmental fate. In some organisms, asymmetric cleavages yield daughter cells that differ in size and appearance, as well as subsequent development. Although we presume that the cytoskeleton is involved in creating these cellular differences, very little is known about which elements of the cytoskeleton are important or how they function.

Early embryogenesis in the nematode *Caenorhabditis elegans* provides a graphic example of the generation of zygotic asymmetry and the production of visibly and developmentally different blastomeres. After fertilization and the completion of meiosis, the zygote undergoes contractions of the anterior membrane and pseudocleavage. Concomitant with pseudocleavage, the pronuclei migrate and meet in the posterior hemisphere, and germ line–specific structures, called "P granules", become localized at the posterior cortex (43, 44). The mitotic spindle for the first division initially lies in the center of the zygote but then becomes asymmetrically positioned (1), leading to an unequal first cleavage. The resulting daughter cells differ not only in size but also in developmental fate, suggesting an asymmetric distribution of developmental potential (9, 24, 44, 45). In previous studies using cytoskeletal inhibitors, we found that P-granule segregation as well as the other manifestations of zygotic asymmetry described above require microfilaments (MFs)[1] but not microtubules (MTs) (44).

Visualization of the distributions of MFs in cells has contributed significantly to our current view of how MFs participate in motility. This applies to the well-known involvement of MFs in muscle contraction, as well as to MF participation in a variety of nonmuscle motility events such as cytokinesis, cytoplasmic streaming, ooplasmic segregation, and organelle transport (6, 16a, 31–33, 35, 39–41, 55). As a first step toward trying to understand how MFs participate in the zygotic motility events described above, I have used rhodamine–phalloidin (R-ph) and anti–actin antibodies to characterize the distribution of MFs in *C. elegans* oocytes and embryos. Concomitant with the intracellular movements that are thought to be MF mediated, the distribution of MFs also

1. *Abbreviations used in this paper*: DAPI, diamidinophenylindole; MF, microfilament; MT, microtubule; R-ph, rhodamine–phalloidin.

Published December 1, 1986

becomes asymmetrically rearranged. This redistribution of MFs is consistent with some models and inconsistent with other models of how MFs could participate in zygotic motility events (see Discussion).

This report also describes the distribution of MFs in the somatic gonad of *C. elegans*. The myoepithelial cells surrounding oocytes may serve several roles: provision of necessary components and spatial cues to the maturing oocytes within (42) and movement of oocytes into the spermatheca for fertilization (47). Consistent with this latter function, the myoepithelial cells contain a striking array of MFs interdigitated with myosin thick filaments.

Materials and Methods

Materials

R-ph was purchased from Molecular Probes, Inc., Junction City, OR and stored as a 3.3-μM stock solution in methanol at −20°C. C4 anti-actin antibody was a gift from Dr. James Lessard (Children's Hospital Research Foundation, Cincinnati, OH). This mouse monoclonal IgG1 was made against actin isolated from chicken gizzard (26). Anti-myosin antibody was a gift from Dr. Jonathan Scholey (University of Colorado, Boulder, CO). This rabbit serum was prepared against calf thymus myosin heavy chain (10). Diamidinophenylindole (DAPI) hydrochloride was obtained from Boehringer Mannheim Biochemicals, Indianapolis, IN. L-lysophosphatidylcholine palmitoyl (lysolecithin) and cytochalasin D were from Sigma Chemical Co., St. Louis, MO.

Nematode Strains and Maintenance

Wild-type (N2) *C. elegans* strain Bristol was cultured at 16°C on agar plates with *Escherichia coli* as food source (5). The actin mutant *st22* (49) was obtained from Dr. Michael Krause (University of Colorado at Boulder) and grown in the same manner.

Fixation of Worms and Embryos

Paraformaldehyde/glutaraldehyde. Gravid adult hermaphrodites were cut open in a small drop of egg salts (118 mM NaCl, 40 mM KCl, 3.4 mM $CaCl_2$, 3.4 mM $MgCl_2$, 5 mM Hepes, pH 7.2; reference 11) on a polylysine-treated microscope slide. A coverslip with a thin layer of high vacuum grease along two edges was placed over the drop. The grease serves to support the coverslip. The coverslip was pressed gently with a toothpick to extrude tissues and embryos from the worm carcasses, after which the solution under the coverslip was replaced with fixative (1.5% wt/vol paraformaldehyde, 0.1% vol/vol glutaraldehyde in embryonic culture medium consisting of 80 mM NaCl, 20 mM KCl, 10 mM $MgCl_2$, 5 mM Hepes, pH 7.2, 50% vol/vol FCS; reference 44). Absorbent paper was used to wick solution underneath the coverslip. Tissues are permeated by fixative without further manipulation, but the eggshells of embryos must be rendered permeable to fixative. Eggshells were cracked by applying further gentle pressure on the coverslip over the embryos with a toothpick. Because oocytes and early-stage zygotes are especially fragile, worms were cut directly into fixative and then pressure permeabilized for studies of these early stages.

Methanol/Acetone. Worms were cut open in a small drop of egg salts on a polylysine-treated slide. A coverslip was placed over the sample, and the slide was immersed in liquid nitrogen for 2 min. The slide was removed from the nitrogen, the coverslip was quickly removed, and the slide was immersed in methanol at 4°C for 10 min, transferred to acetone at 4°C for 10 min, rinsed in H_2O, and finally washed in PBS, pH 7.4 (150 mM NaCl, 3 mM KCl, 8 mM Na_2HPO_4, 1.5 mM KH_2PO_4, 1 mM $MgCl_2$).

Staining of Worms and Embryos

Method I (R-ph). A rapid one-step fixation/permeabilization/staining procedure (similar to that suggested by Molecular Probes, Inc.) was usually used for R-ph visualization of MFs. The paraformaldehyde/glutaraldehyde fixative described above contained 0.33 μM R-ph and 0.5 mg/ml lysolecithin. Samples were fixed and stained for 20–30 min at room temperature and sometimes transferred to 4°C for storage for several hours (without any noticeable affect on staining). Samples were washed by wicking PBS underneath the coverslip. The DNA in cells was stained by including DAPI at 0.5–1 μg/ml in one of the PBS washes. The coverslip was sealed to the slide using nail polish, and samples were observed and photographed immediately.

Method II (R-ph). In this second procedure, fixation and staining were carried out separately. Samples were incubated in 1.5% paraformaldehyde, 0.1% glutaraldehyde in culture medium for 20 min at room temperature, followed by (*a*) a 20–30-min incubation in 0.33 μM R-ph and 0.5% Triton X-100 in culture medium, or (*b*) a 20–30-min incubation in 0.5% Triton X-100 in culture medium and then 20–30 min in 0.33 μM R-ph in culture medium. Samples were washed and DAPI stained as in Method I. Postfixation staining resulted in fluorescence patterns similar to those seen with the one-step method, but there was more variability in the degree of penetration of R-ph into embryonic blastomeres when staining was carried out after fixation.

Method III (Anti-actin). The specificity of the anti-actin antibody for nematode actin was verified by Western immunoblot analysis. Worms were homogenized in boiling gel sample buffer and the worm proteins separated by PAGE. After transfer of the proteins to nitrocellulose, only a single component of appropriate molecular weight was recognized by the antibody (data not shown). For staining with the antibody, worms were cut and fixed with paraformaldehyde/glutaraldehyde as described above. Sometimes 0.5 mg/ml lysolecithin was included in the fix. This resulted in less variability in antibody penetration and improved visualization of fluorescence signal above background, perhaps due to extraction of G-actin and other soluble components (30). After fixation for 20 min at room temperature, the coverslip was removed, and the samples were permeabilized by incubation in methanol at 4°C for 10 min, followed by acetone at 4°C for 10 min, rinsed in H_2O, and washed in PBS. Each sample was incubated with 30 μl of 1.5% ovalbumin/1.5% BSA in PBS for 1 h at room temperature, followed by 30 μl of C4 anti-actin antibody (diluted to 20 μg/ml in PBS) for 6–12 h at 4°C. The slides were washed in PBS at 16°C for 1 h and incubated for

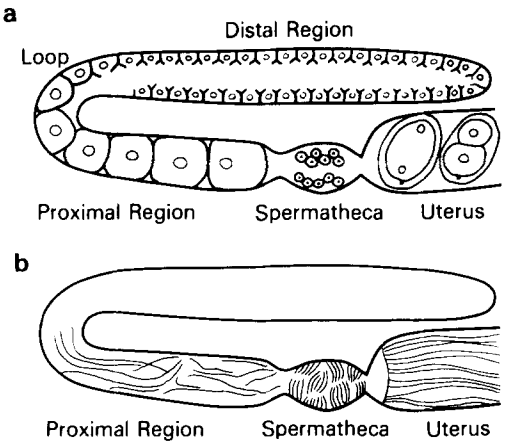

Figure 1. Diagrams of one of the two gonad arms in an adult hermaphrodite worm. (*a*) Central longitudinal section showing the germ cells inside the gonad. In the distal region, the germ nuclei are located around the periphery of the tube-like organ in membrane cubicles that are open at their inside edges. Thus the germ nuclei are in a common cytoplasm. The germ nuclei enter meiosis in the distal region and become completely enclosed in membrane just before the loop. Oocytes mature and enlarge as they move through the proximal region toward the spermatheca, where fertilization takes place. A zygote and 2-cell embryo are shown in the uterus. The somatic gonad cells form a very thin layer around the germ nuclei and oocytes, and enclose sperm and embryos in the spermatheca and uterus, respectively. This layer of somatic tissue is represented by the thick line surrounding the germ cells. (*b*) Top or bottom surface of the gonad illustrating the arrangement of actin fibers in the somatic gonad (see Figs. 2 and 3). It is difficult to discern the cell boundaries of the myoepithelial cells of the proximal region and the uterine cells. Both of these tissues contain MFs that run longitudinally. The spermatheca is composed of distinct polygonal cells containing MFs that run circumferentially around the spermatheca.

Published December 1, 1986

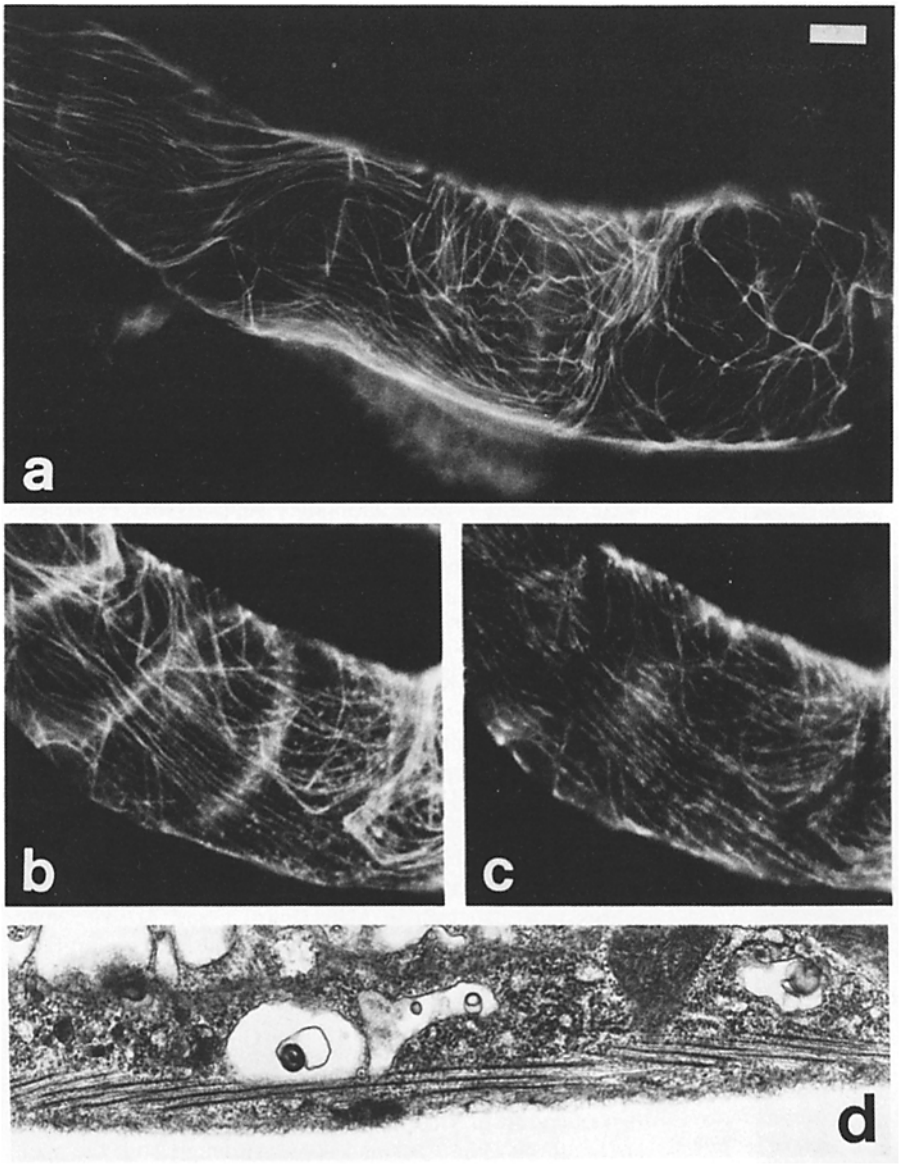

Figure 2. Actin and myosin filament arrays in the somatic cells of the proximal region of the gonad. Gonads were cut out of hermaphrodites and (*a*) simultaneously fixed and stained with R-ph by Method I or fixed and double labeled with (*b*) anti-actin and (*c*) anti-myosin using Method IV. Actin and myosin-containing filament bundles run roughly longitudinally from the loop of the gonad (*left*) to the spermatheca (*right*), as diagrammed in Fig. 1 *b*. (*d*) Electron micrograph of interdigitated thick and thin filaments in a longitudinal section of the proximal region. Bar, 10 μm.

6–12 h at 4°C with 30 μl FITC-conjugated goat anti-mouse IgG serum (United States Biochemical Corp., Cleveland, OH) diluted 1:100 in PBS. The slides were washed in PBS at 16°C for 90 min (DAPI at 0.5 μg/ml was included in one of the PBS washes), rinsed with H_2O, and mounted in Gelutol (Monsanto Co., St. Louis, MO) mounting fluid.

Method IV (Anti-actin and Anti-myosin). The reactivity of the anti-myosin antibody with worm myosin was confirmed by Western immunoblots (data not shown; also, Lye, J., University of Colorado, personal communication). Worms and embryos were fixed in methanol/acetone as described above. Samples were stained as described in Method III, including anti-thymus myosin antibody (diluted 1:100) in the primary antibody incubation, and rhodamine isothiocyanate-conjugated goat anti-rabbit IgG serum (United States Biochemical Corp.) in the secondary antibody incubation.

Treatment of Tissues and Embryos with Cytochalasin D

Cytochalasin D was stored as a 2 mg/ml stock solution in 95% EtOH at 4°C and diluted in embryonic culture medium immediately before use. Worms were cut open and pressed to extrude tissues and embryos, as described for paraformaldehyde/glutaraldehyde fixation. The solution under the coverslip was replaced with cytochalasin D–containing medium, and embryos were pressure permeabilized. After incubation for 1–15 min at room temperature, samples were fixed and stained with R-ph or anti-actin, as described.

Photography

A Zeiss Photomicroscope III equipped with epifluorescence optics was used for observation and photography. Examination was done with a 40× Neofluar or a 63× Planapochromat (oil) objective. Kodak Tri-X film was exposed at ASA 800–6,300 and developed in Diafine Two-Bath Developer (Acufine, Inc., Chicago, IL). Embryos were photographed first with 515–560-nm epi-illumination to visualize rhodamine fluorescence or 450–490-nm epi-illumination to visualize fluorescein fluorescence, and then with 365-nm epi-illumination to visualize DAPI-stained DNA. In all photographs, embryos are oriented anterior-left, posterior-right.

Electron Microscopic Visualization of Thick and Thin Filaments

Worms were cut open in M9 salts (5) and transferred to a test tube containing 2.5% glutaraldehyde, 0.1 M Na cacodylate, pH 7.2, 1 mM $MgCl_2$. Tissues were fixed for 1 h at room temperature and then at 4°C for several hours to several days. Tissues were rinsed three times in 0.1 M cacodylate buffer, postfixed in 1% OsO_4 in cacodylate buffer for 30 min at 4°C, rinsed three times in H_2O, mounted in agar, stained with 0.5% uranyl acetate in H_2O, dehydrated in a graded EtOH series, embedded in DER resin, and sectioned. Sections were stained in a 50:50 mixture of 7.5% aqueous uranyl-

Published December 1, 1986

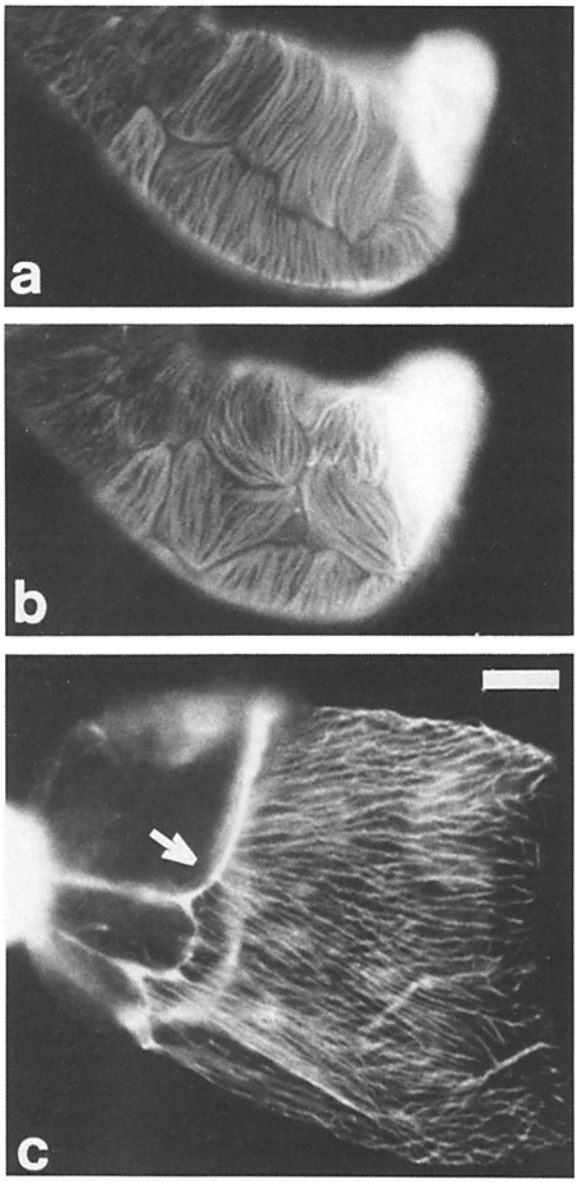

Figure 3. Microfilaments in the somatic cells of the spermatheca and uterus. Gonads were cut out of hermaphrodites and simultaneously fixed and stained with R-ph (Method I). (*a* and *b*) Top and bottom surface of the spermatheca showing polygonal cells containing aligned MF bundles (see Fig. 1 *b*). The valve from the spermatheca to the uterus (*upper right*) stains intensely. (*c*) Aligned MF bundles in the uterus (see Fig. 1 *b*). These extend from what looks like an MF lariat (*arrow*) attached to the spermatheca (*left*). Bar, 10 μm.

magnesium acetate and 95% EtOH for 30 min, followed by lead citrate for 5 min, and examined with a Philips 300 electron microscope.

Results

Microfilament Distribution in the Somatic Gonad

The gonad in an adult hermaphrodite worm is a double-armed organ composed of germ cells surrounded by a somatic sheath (17, 21). The distal region of each arm contains a central core of cytoplasm surrounded by a cylindrical layer of germ nuclei that are partially enclosed in membrane (Fig. 1 *a*). The germ nuclei near the distal tip divide mitotically and then enter meiosis (17). Oocytes form at the loop and move through the proximal region to the spermatheca. The somatic sheath surrounding the germ cells is a monolayer composed of 10 cells per gonad arm (21). The region of this sheath around the oocytes (six sheath cells per gonad arm) is visibly contractile; contractions result in shortening of the proximal region, which appears to force the oocytes within the sheath into the spermatheca (21, 47). Staining of the contractile somatic gonad cells with either R-ph (51, 52, 54) or anti-actin antibodies reveals an unusual array of MF bundles (Figs. 1 *b* and 2, *a* and *b*). The bundles run roughly longitudinally, from loop to spermatheca, although they sometimes zigzag and often curve to run circumferentially for a short distance.

Simultaneous staining of the gonad sheath cells with anti-actin and anti-myosin antibodies supports the hypothesis that contraction of these cells is an actomyosin-mediated process (17). Anti-myosin stains the same fiber bundles that anti-actin does, but the staining pattern is more periodic than anti-actin or R-ph (Fig. 2, *b* and *c*). (As an internal control for the specificity of staining by each antibody, muscle tissue was examined. It was observed that anti-actin stains I bands and anti-myosin stains A bands only.) The interdigitation of actin thin filaments and myosin thick filaments is seen by electron microscopic examination of longitudinal sections of the somatic gonad (Fig. 2 *d*; also see gonad cross-section in reference 17). Thus this myoepithelial layer contains actin and myosin filaments that may interact to cause contraction.

Two other somatic gonad tissues, the spermatheca and the uterus, are also rich in MFs (Figs. 1 and 3). The spermatheca, in which sperm are housed and fertilization takes place (47), is made up of polygonal cells containing densely packed and aligned MFs that run approximately circumferentially around the spermatheca (Figs. 1 *b* and 3, *a* and *b*). The uterus, which extends between the two spermathecae and contains fertilized eggs, contains aligned MF bundles that extend from what looks like an MF lariat attached to the spermatheca (Figs. 1 *b* and 3 *c*). Although both the spermatheca and uterus are contractile tissues (21, 47; S. Ward, Carnegie Institute of Washington, personal communication), the anti-myosin antibody used in these studies does not stain either the spermathecal or uterine fiber bundles.

Microfilaments in Germ Cells

In the distal portion of the gonad, R-ph stains MFs along the membranes that surround the germ nuclei. The germ nuclei are located around the periphery of the gonad and are incompletely enclosed in membrane (see Fig. 1 and reference 17). By focusing on the mid-focal plane of the distal region, the cubicle arrangement of membrane invaginations and MFs around germ nuclei can be seen (Figs. 1 *a* and 4, *c* and *d*). Focusing on the top or bottom surface reveals the honeycomb arrangement of membrane cubicles and MFs (Fig. 4, *a* and *b*). At the loop of the gonad, germ nuclei become completely enclosed in membrane, forming oocytes (Fig. 1 *a*). As seen in Fig. 4, R-ph stains around the periphery of newly formed and maturing oocytes. R-ph staining can be better visualized when gonads are cut to release oocytes (see below).

Published December 1, 1986

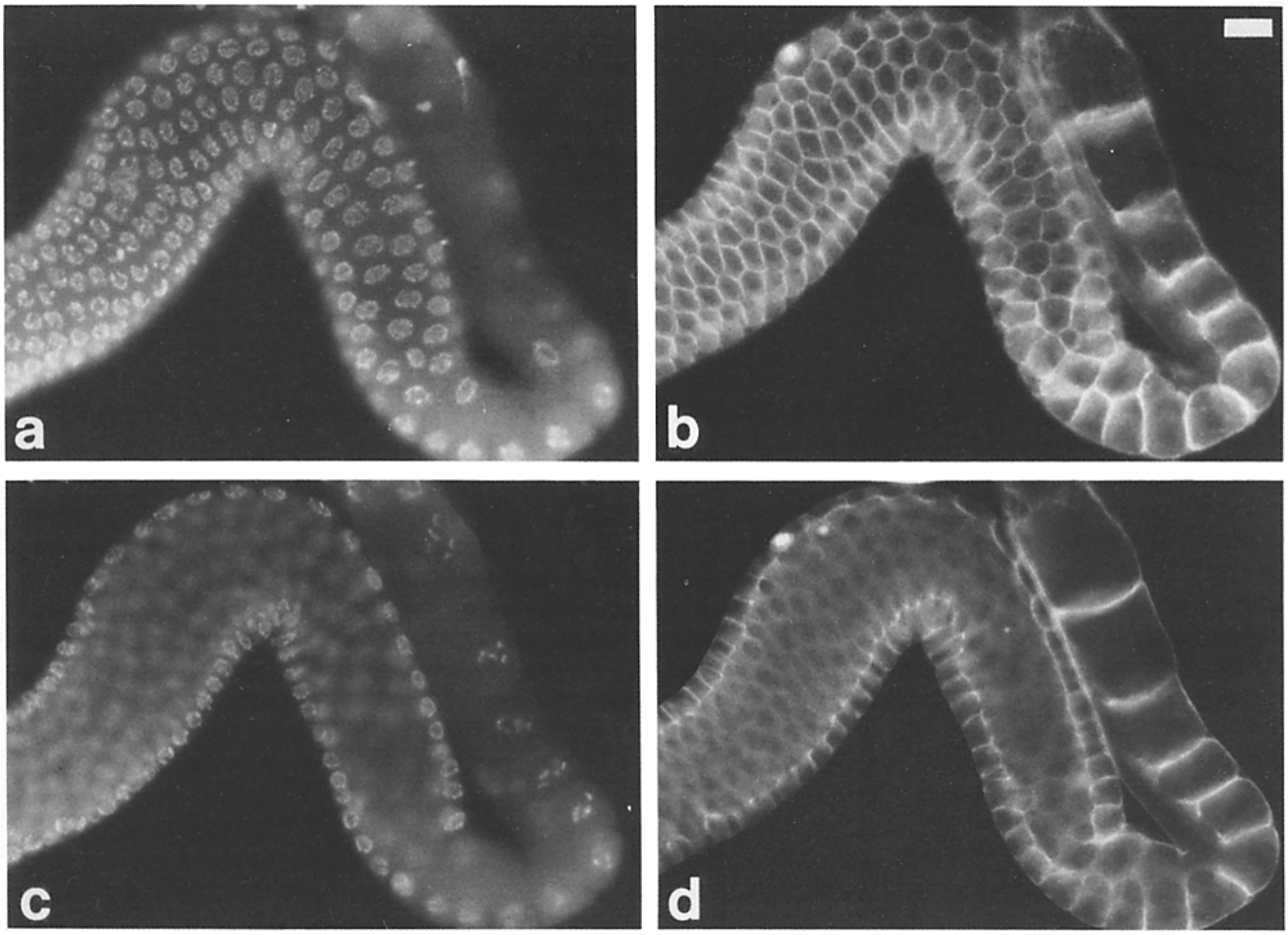

Figure 4. R-phalloidin staining of germ cells in the gonad. Gonads were cut out of hermaphrodites and stained with R-ph (Method II). The upper panels show an upper surface of the gonad. (*a*) DAPI-stained nuclei. (*b*) R-ph-stained MFs. The lower panels show a mid-focal plane through the same gonad, similar to that shown in Fig. 1 *a*. (*c*) DAPI. (*d*) R-ph. R-ph stains MFs along the membranes that surround the germ nuclei. The membrane cubicles are arranged like a honeycomb in the distal region (left side of each panel). Oocytes form at the loop and enlarge in the proximal region (right side of each panel). Bar, 10 μm.

Microfilaments in Oocytes and Embryos

The distribution of MFs in oocytes and early embryos is complex and varies with developmental stage. The most striking features of the MF pattern are shown in Fig. 5. F-actin appears to exist in two cortical arrangements: fibers and dots or foci. In oocytes and newly fertilized zygotes, one gets the impression of a fibrous network, although distinct fibers are difficult to visualize; fibers are clearly observed in later stage zygotes (Fig. 5). The actin dots, which are observed at all stages, undergo a remarkable reorganization partway through zygote development; they become concentrated in the anterior hemisphere of the zygote (Fig. 5). A more detailed description of MF patterns as a function of developmental stage is presented below.

In oocytes released from gonads, R-ph stains a cortical meshwork that appears mainly granular (Fig. 6 *a*). In the microscope, it appears as if there is a fibrous network as well, but this has been difficult to capture on film. The cortical staining pattern is uniform; there are no obvious regions of concentrated MFs or regions devoid of MFs.

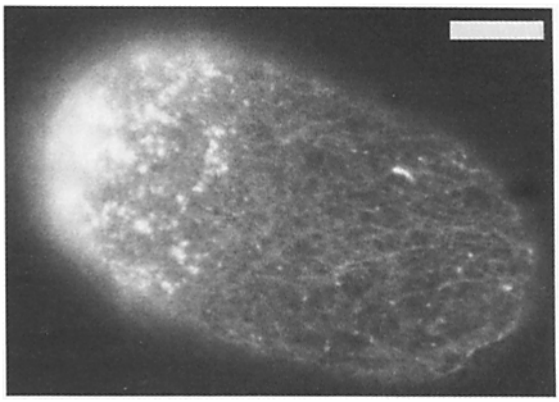

Figure 5. Actin fibers around the periphery and actin foci concentrated in the anterior end of a zygote at pronuclear meeting. Embryos were cut out of hermaphrodites and simultaneously fixed and stained with R-ph (Method I). This view of the top surface was seen using a 63× oil objective. The foci of actin are over-exposed so that the fibers can be seen. Bar, 10 μm.

Published December 1, 1986

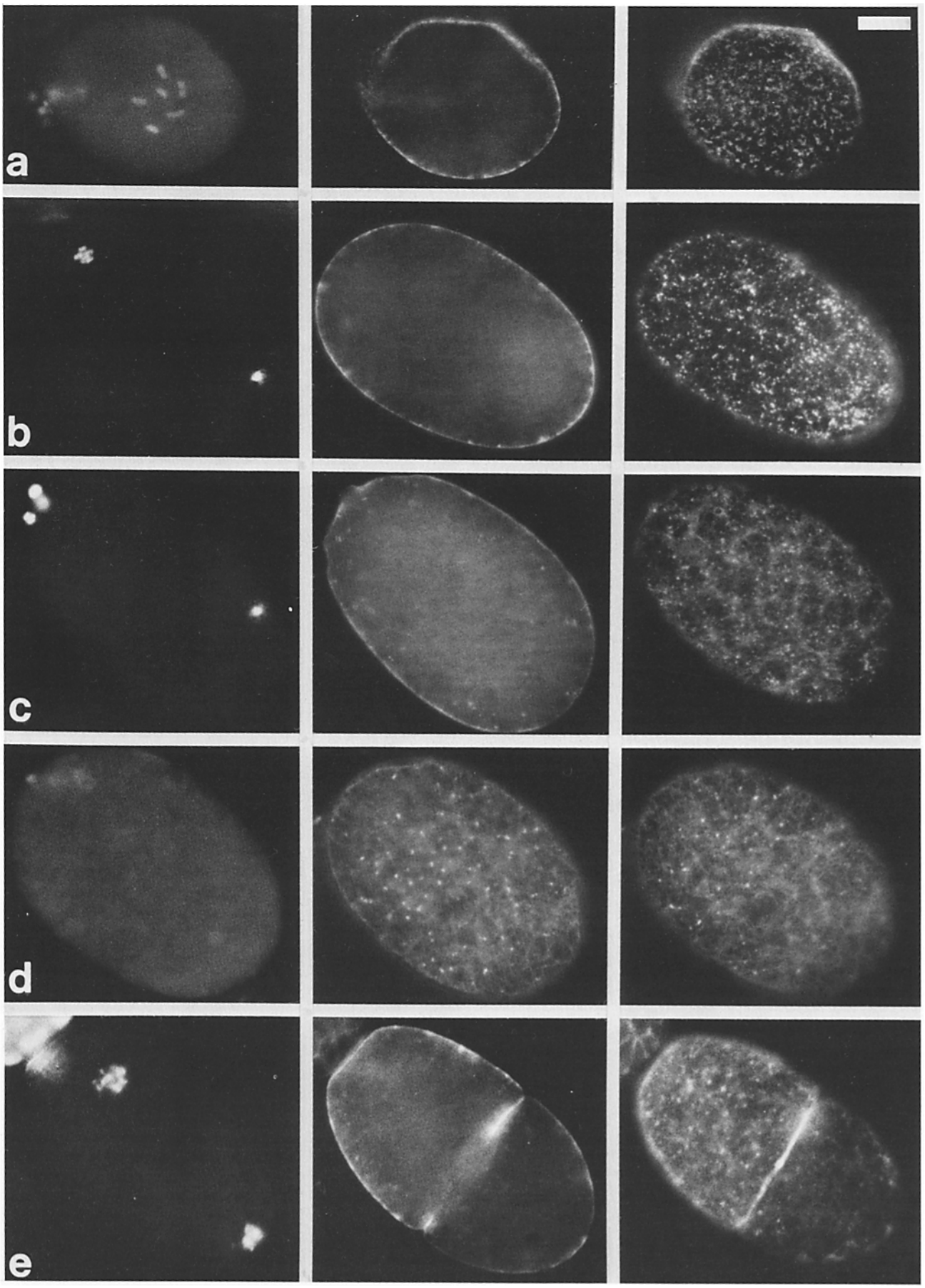

Published December 1, 1986

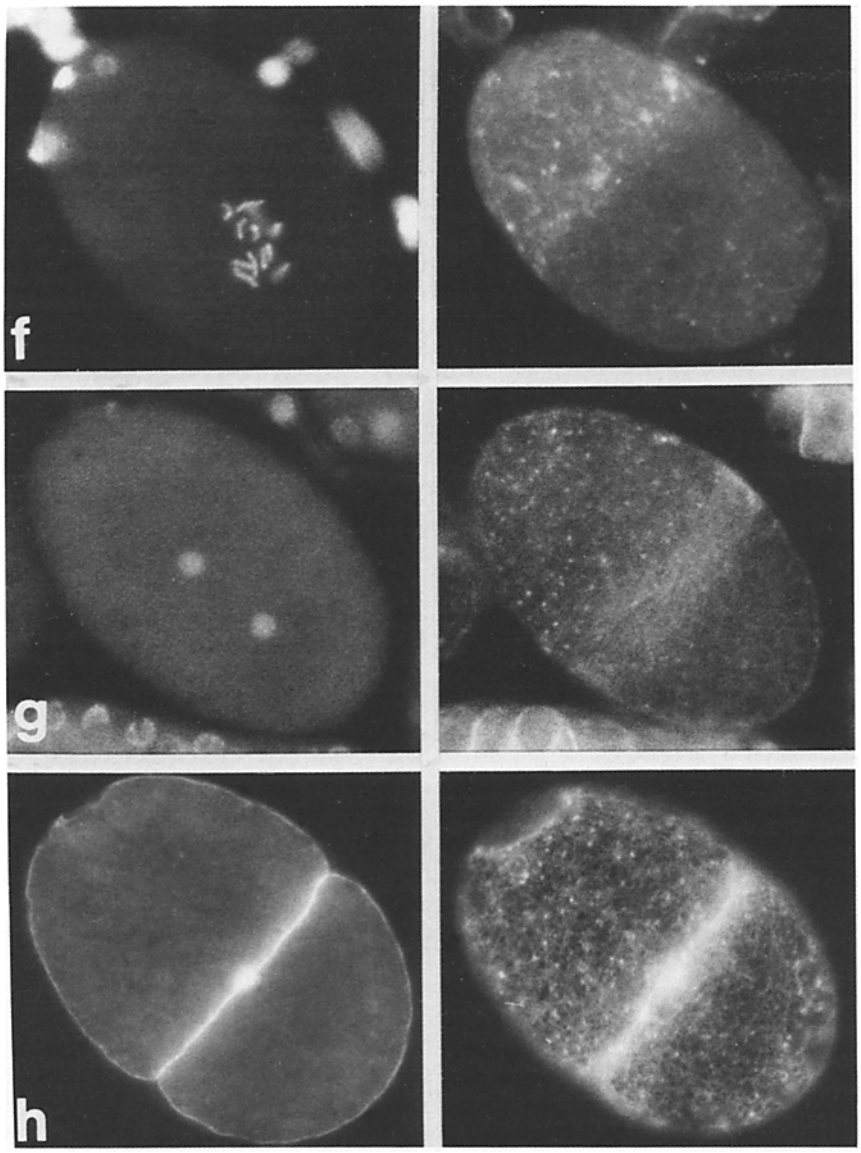

Figure 6. R-phalloidin staining of fibers and dots in oocytes and early embryos. Oocytes and embryos were cut out of hermaphrodites and simultaneously fixed and stained with R-ph (Method I). The left panel of each set (except *h*) shows DAPI-stained chromosomes. The middle and right panels show R-ph staining seen at mid-focal planes and on the top surface. All embryos are oriented anterior-left, posterior-right. (*a*) Oocyte, showing the granular nature of the surface stain. (*b*) Zygote during meiosis I. The surface staining by R-ph is still mainly granular. (*c*) Zygote during meiosis II. R-ph stains a meshwork of fibers. Dots or foci of actin are located within the meshwork and somewhat deeper as well. (*d*) Zygote during formation of the pronuclei. The middle panel shows R-ph staining of foci just below the meshwork of fibers. The right panel shows the foci within the meshwork beginning to clear from the posterior end. (*e*) Zygote during pronuclear migration and pseudocleavage. R-ph stains the pseudocleavage furrow. The foci of actin are becoming more concentrated in the anterior hemisphere (*right panel*). (*f*) Zygote at pronuclear meeting, showing the localization of foci anterior. Actin fibers persist around the entire periphery (see Fig. 5). (*g*) Zygote at telophase of first mitosis. Foci of actin remain anterior as MFs align circumferentially around the zygote where the cleavage furrow will form. (*h*) Two-cell embryo showing the cortical meshwork of fibers and foci. Both panels show R-ph staining, at a mid-focal plane (*left panel*) and on the top surface (*right panel*). Bar, 10 μm.

Based on observation using Nomarski DIC microscopy, the *C. elegans* zygote displays polarity immediately after fertilization; the site of sperm entry is posterior. The oocyte nucleus, located at the end opposite the sperm, completes meiosis and extrudes two polar bodies. The polar bodies serve as anterior markers. R-ph staining of newly fertilized zygotes results in a pattern of surface staining similar to that seen in oocytes; a granular meshwork that appears to contain very fine, indistinct fibers (Fig. 6 *b*). There is no marked concentration of MFs at the site of sperm entry (posterior) or at the zygote surface where polar bodies are extruded (anterior). As meiosis progresses the fibrous nature of the surface staining becomes more pronounced. Dots or foci of actin are seen throughout the cortical meshwork and somewhat deeper as well (Fig. 6 *c*).

The homogeneous distribution of fibers and foci in the zygote begins to change during pronuclear migration and pseudocleavage. As described previously, these events are the first of a series of directed movements that reflect the asymmetry of the zygote and lead to the production of blastomeres that differ in size and developmental fates. During this critical period, the anterior membrane contracts and a pseudocleavage furrow is formed and resorbed. The maternal pronucleus migrates to meet the paternal pronucleus in the posterior hemisphere of the zygote. Concurrently germ line–specific P granules become localized in the posterior cytoplasm destined for the posterior blastomere P1 (44). R-ph staining of zygotes during this period reveals that, although the meshwork of fibers persists around the periphery of the zygote, the foci of actin become progressively more concentrated in the anterior hemisphere (Figs. 5 and 6, *d–f*). The pseudocleavage furrow also stains with R-ph during this period (Fig. 6 *e*).

The foci of actin remain anterior as the zygote generates an asymmetric mitotic spindle and undergoes karyokinesis, at which time actin fibers align circumferentially around the zygote where the cleavage furrow will form (Fig. 6 *g*). During cytokinesis the cleavage furrow is very brightly stained by R-ph. Immediately after cleavage, the larger anterior cell (AB) contains a cortical meshwork of fibers and foci and the smaller posterior cell (P1) contains a cortical meshwork with very few foci. Foci do appear in P1 later, and, in fact, cortical

Published December 1, 1986

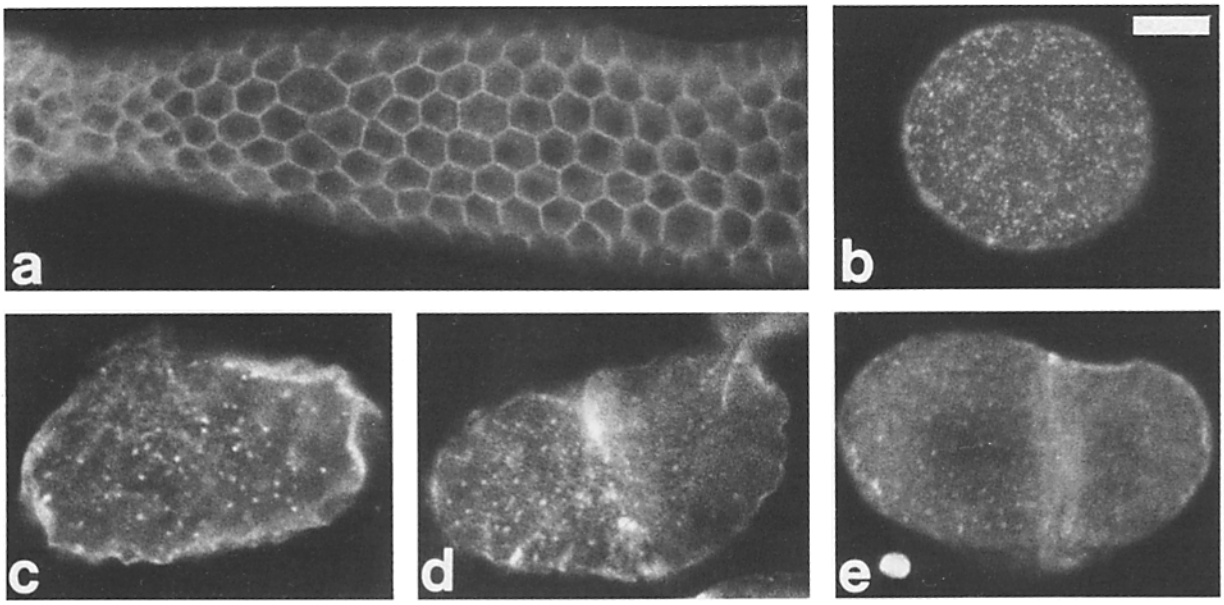

Figure 7. Anti-actin staining of microfilaments in the distal gonad, oocytes, and zygotes. Gonads and embryos were cut out of hermaphrodites and fixed and stained using Method III for *a–d* and Method IV for *e*. (*a*) Upper surface of the distal gonad. This corresponds to the R-ph staining seen in Fig. 4 *b*. (*b*) Upper surface of an oocyte, showing particulate staining similar to that seen with R-ph in Fig. 6 *a*. (*c*) Zygote during meiosis, showing staining of foci of actin in the cortex, corresponding to the zygote shown in Fig. 6 *c*. (*d*) Zygote during pronuclear migration and pseudocleavage, showing anti-actin staining of the pseudocleavage furrow and of anteriorly localized foci, as seen with R-ph in Fig. 6 *e*. (*e*) Zygote at anaphase of first mitosis, showing foci of actin localized anteriorly and fibers aligned circumferentially around the zygote, as seen with R-ph in Fig. 6 *g*. Bar, 10 μm.

fibers and foci are characteristic of the blastomeres of early-stage embryos, when the top or bottom surfaces of the cells are examined (Fig. 6 *h*). When viewed through a central focal plane, the cortical fibers and foci appear as bright surface stain, especially bright between blastomeres, probably due to the flattening of cells against each other and therefore more surface area at junctions (Fig. 6 *h*).

Staining of oocytes and zygotes with anti-actin antibodies results in MF patterns similar to those seen with R-ph (Fig. 7). In general, anti-actin gives fainter staining than R-ph, and embryos often appear misshapen after the pressure treatment required to permeabilize them to molecules as large as antibodies (see Materials and Methods for details). Even with these drawbacks, the antibody staining has corroborated the existence of fibers and foci and the anterior localization of foci. It has not been possible to investigate the localization of myosin relative to the array of MFs in zygotes because the anti-myosin antibody used in these studies does not stain embryos.

Effects of Cytochalasin D on Microfilament Patterns

To examine the sensitivity of the MF fibers and foci to MF inhibitors, zygotes were treated with cytochalasin D (46) before fixation and staining with R-ph or anti-actin. Cytochalasin D at 1 μg/ml resulted in loss of the cortical meshwork of fibers and foci and the appearance of large aggregates of stained material throughout the cytoplasm (Fig. 8). These apparent aggregates of F-actin were seen within 1 min of exposure to cytochalasin D and were present even when embryos were treated with much higher concentrations of cytochalasin D (up to 20 μg/ml) or for longer periods before fixation (up to 15 min; data not shown).

The bundles of MFs in the somatic gonad were not noticeably affected by exposure to cytochalasin D, at concentra-

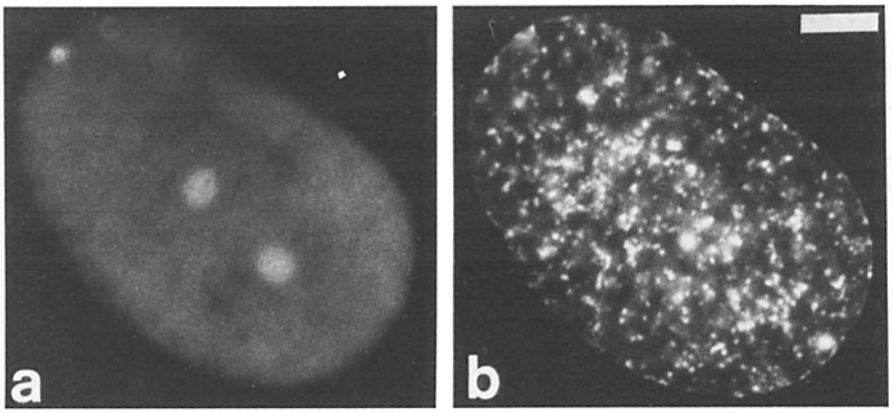

Figure 8. R-ph staining of a zygote treated with cytochalasin D. This embryo was rendered permeable to 1 μg/ml cytochalasin D and stained with R-ph (Method I) 8 min later. (*a*) DAPI image. The embryo is at anaphase/telophase of first mitosis. (*b*) R-ph stains aggregates and sometimes spikes of F-actin distributed throughout the cytoplasm. Bar, 10 μm.

Published December 1, 1986

tions up to 20 μg/ml (data not shown). This did not appear to be due to poor permeation of the drug because free fibers fortuitously extruded from the ends of cut gonads were intact, and somatic gonad fibers were stable when the oocytes within were clearly affected. Thus the bundles of actin filaments in the somatic gonad resemble the sarcomeric filaments in muscle in their stability to MF inhibitors.

Effects of an Actin Mutant on Microfilament Patterns

There are four actin genes in *C. elegans*: actins 1–3 are clustered on chromosome V and are proposed to be muscle actins (14, 22, 49, 50); actin 4 is on the X-chromosome (2). Mutations in the cluster of three actin genes are dominant; mutant worms are uncoordinated and contain very disorganized muscle thin filaments (49). One of these dominant mutants, *st22* (in actin 3; reference 49) was used to investigate whether the actin subunits encoded by a "muscle" actin gene normally participate in the structures described in this report. The MF bundles in the somatic gonad are somewhat affected in homozygous *st22* worms: a fairly normal array of MF bundles runs through the somatic gonad cells, but the bundles are seen to aggregate in a manner not seen in wild-type worms (data not shown). This result suggests that the somatic gonad fibers are at least partially composed of "muscle" actin subunits. The patterns of MF staining around the germ nuclei, in oocytes, and in embryos are not visibly affected in *st22* mutants (data not shown). This result suggests that at least one of the muscle actins (actin 3) is not involved in these structures or that, if involved, aberrant subunits do not interfere with MF organization in these tissues as they do in muscle.

Discussion

Visualization of Microfilaments

An accurate description of the distribution of molecules in cells relies on a method of fixation that preserves the distribution present in living cells. To characterize a molecule's distribution by fluorescence, a probe that is specific for the molecule must be used. The evidence that the distributions of MFs described in this report represent the distributions in vivo is the following: (*a*) Similar MF patterns are seen in tissues prepared by a variety of fixation/permeabilization protocols (see Materials and Methods for details). For most experiments, samples were fixed with a mixture of paraformaldehyde and glutaraldehyde; paraformaldehyde is thought to penetrate tissue rapidly, while glutaraldehyde is thought to fix tissue more effectively (34). Sometimes lysolecithin was included in the fixative to promote penetration of the aldehyde and R-ph and allow soluble components to be partially extracted (30). As an alternative to aldehydes, samples were also fixed in methanol/acetone. (*b*) Two different actin probes, R-ph and anti-actin antibodies, result in similar patterns of staining. R-ph is specific for filamentous or F-actin (51, 52, 54), and the anti-actin antibody used sees both G-actin and F-actin (26; unpublished observation). (*c*) As an internal control, in fixed worm samples, R-ph and anti-actin stain muscle and the gut lumen, both of which are known to contain MFs by electron microscopy (49, 50; unpublished observation). (*d*) The MF distributions in germ cells and embryos are sensitive to the MF inhibitor, cytochalasin D (46). The cytochalasins prevent actin filament elongation by binding to the fast polymerizing end of actin filaments (15, 27). I used cytochalasin D because it has a higher affinity for actin than does cytochalasin B and does not interfere with hexose transport, as does cytochalasin B (15, 46).

Although every effort was made to control for artifactual redistribution of MFs during fixation and staining, the possibility remains that some aspects of the MF pattern described are artifactual. Especially suspect are the foci seen in embryos, since foci are not a common actin configuration. However, the possibility that the foci are artifacts does not diminish the importance of the finding that fixable actin becomes asymmetrically localized during a critical time in zygote development.

Microfilaments in Oocytes and Zygotes

An important aspect of early embryonic development in all organisms is the rearrangement of cytoplasmic components that occurs after fertilization. Studies of embryos treated with cytoskeletal inhibitors demonstrate that MFs and MTs are involved in many of the different intracellular movements that have been studied (19, 28, 29, 35–38, 44, 55). For this reason it is important to understand what cytoskeletal components the oocyte contains, how these components are arranged, and how the distribution changes after fertilization.

MFs are present at the cortex of *C. elegans* oocytes and early embryos, as in many other organisms. These MFs exist as a meshwork of fine fibers and foci. The existence of fibers of actin is consistent with the state of this polymer in many other eukaryotic cell types. The existence of foci or dots of actin, while somewhat unusual, is likely to be real; as discussed above, foci are seen with both R-ph and anti-actin in embryos fixed by different procedures. The foci are not likely to be microvilli; microvilli have not been seen in electron micrographs of fixed *C. elegans* embryos (53). Actin dots are not unique to *C. elegans*; they are also observed in mouse embryos (25), in Drosophila embryos (48), in the fungi yeast and Uromyces (18, 20), and in transformed cells (4, 7).

In the oocyte, MFs do not appear to be concentrated in or missing from any regions of the cortex in a way that indicates asymmetry or predicts a predetermined region of sperm entry. After fertilization, the distribution of MFs remains uniform over the entire surface as the egg nucleus completes meiosis, in contrast to the concentration of MFs observed at the surface over the sperm and egg pronuclei in newly fertilized mouse zygotes (28, 29).

The first visible reorganization of MFs in *C. elegans* zygotes is observed after the completion of meiosis as the pronuclei form and migrate. From previous studies it is known that this migration is temporally accompanied by contractions of the anterior membrane, formation and resorption of a pseudocleavage furrow, and segregation of germ line–specific P granules to the posterior cortex (44). During this period the foci of MFs become progressively more concentrated in the anterior cortex. This appears to occur by clearing of foci from progressively more of the posterior end of the zygote. Whether this is due to movement of most of the foci in an anterior direction or disassembly of most of the posterior foci is not known.

Published December 1, 1986

Review of the Evidence for Microfilament Involvement in the Generation of Zygotic Asymmetry

In previous studies (44), we found that disruption of MFs by treatment of *C. elegans* zygotes with MF inhibitors (cytochalasin D or B) prevents the zygotes from manifesting the aspects of asymmetry that we can monitor. Contractions of the anterior membrane and pseudocleavage do not occur. Pronuclear migration occurs, but the two pronuclei meet in the center of the zygote instead of the posterior hemisphere. P granules do not become localized at the posterior cortex but instead coalesce into a tight cluster near the center of the inhibited zygote. The spindle does not become asymmetric in its position along the A-P axis, and the two poles of the spindle do not appear or behave differently, as they do in normal zygotes. In contrast, eliminating MTs by treating zygotes with MT inhibitors (colcemid, vinblastine, or griseofulvin) inhibits pronuclear migration but does not appear to affect pseudocleavage or P-granule segregation. Therefore, MFs, but not MTs, appear to be required for the zygote to be able to manifest asymmetry.

A Model for Microfilament Participation in Asymmetric Zygotic Movements

The present studies were undertaken to test the three most obvious models for MF participation in the asymmetric segregation of P granules: (*a*) movement of P granules along oriented bundles of MFs, similar to the myosin-mediated translocation of vesicles along MF bundles in *Chara* and *Nitella* (41); (*b*) pulling of P granules posteriorly by aggregation of MFs in the posterior end of the zygote, similar to ooplasmic segregation of myoplasm in ascidian zygotes (19, 35); and (*c*) pushing of P granules posteriorly by aggregation of MFs in the anterior end of the zygote. The observed distribution of MFs does not support the first two models; oriented bundles of MFs are not seen, and there is not a massive contraction of actin to the posterior end of the zygote. Rather, the observed distribution of MFs is most consistent with the third model.

Taken together, the results of the inhibitor studies (44) and MF staining suggest the following hypothetical picture of zygote development. The foci of actin may represent part of a contractile network. Contractions of the anterior membrane are seen as the foci become concentrated in the anterior cortex of the zygote. These contractions may push cytoplasmic components, such as P granules and the egg pronucleus, in a posterior direction. The anterior network of actin foci may participate in generating an asymmetric spindle by holding the anterior aster immobile while the posterior aster moves posteriorly and swings. (Euteneuer and Schliwa recently reported evidence for an interaction between actin and MTs radiating from centrosomes, leading to an involvement of MFs in determining the position of the centrosome [13].) Finally MFs probably participate in cytokinesis in a manner similar to other eukaryotic cells (39, 40), by aligning circumferentially in the cortex and presumably interacting with myosin to draw the cleavage furrow closed.

An alternative possibility is that the foci do not participate in generating asymmetry but instead respond to the asymmetry of the zygote and are segregated anteriorly. In addition, the fact that P granules form a tight cluster in the center of cytochalasin-treated zygotes suggests a further possibility: P granules may be attached to an as yet unidentified contractile network that contracts to the center of the zygote upon cytochalasin treatment. Future experiments on mutant and manipulated embryos should elucidate the interrelationship of MFs and early movements and events.

Analysis of Microfilaments in Embryos from an Actin Mutant

It has been proposed that the cluster of three actin genes on chromosome V encode muscle actins and the single actin gene on the X-chromosome encodes the cytoplasmic actin found in nonmuscle cells of the worm (14, 22, 49). This hypothesis is supported by the observation that mutations in the actin cluster affect functions like movement and pharyngeal pumping; they do not appear to affect nonmuscle functions such as cytokinesis, which would probably result in lethality. The lack of detectable effects of a dominant mutation in the actin cluster on MFs in embryos is consistent with the above hypothesis. Mutations in the X-linked actin gene, actin 4, have not been identified. Isolation of such mutations should shed light on the overlap in use of actin subunits in muscle and nonmuscle cells.

Microfilaments in the Somatic Gonad

The somatic gonad arises from the lineage (MS, reference 21) that produces most of the muscle in the worm. The somatic cells surrounding the proliferating germ nuclei in the distal portion of the gonad seem to serve purely as a sheath; MF arrays are not seen and it does not contract. The somatic cells that surround the developing oocytes, on the other hand, are myoepithelial; longitudinal bundles of interdigitated thick and thin filaments apparently endow these cells with contractility. This myoepithelium resembles striated muscle in the orderliness of the lateral arrangement of thick and thin filaments (16a, 33, 50). However, the myoepithelial filaments are not organized into the repeating sarcomeres typical of striated muscle; in this respect, the myoepithelium resembles vertebrate smooth muscle, vertebrate myoepithelium, and stress fibers in cultured cells (6, 12, 16, 16a, 33).

The structural organization of myofilaments in vertebrate smooth muscle, myoepithelium, and stress fibers is not well understood. However, all of these cell types contain electron-dense bodies that resemble the Z lines of striated muscle (3, 6, 12, 16, 16a). Studies of the polarity of the MFs inserted into the dense bodies (3) and the arrangement of myosin relative to the dense bodies (23) suggest that the myofilaments in these cell types may, in fact, be arranged as sarcomeres, although more loosely constructed. The periodic staining of myosin along actin fibers in *C. elegans* myoepithelium is consistent with a sarcomere-like organization.

Given the similarities and differences between myoepithelium and muscle filaments in worms, it was of interest to determine whether the thin filaments in the gonad represent a novel configuration of "muscle" actin or are composed of actin encoded by different genes than the actin found in muscle cells. Based on the effect of the *st22* mutation in actin 3 on somatic gonad fibers, it appears that these fibers do contain at least some "muscle" actin. Therefore the fibers in the gonad seem to resemble muscle thin filaments in their use of

Published December 1, 1986

"muscle" subunits, their interdigitation with myosin thick filaments, their contractile role, and their stability to MF inhibitors. However, their association with myosin appears less ordered than the sarcomeric configuration seen in muscle.

Finally, an observation by Ward and Carrel (47) suggests an intriguing interaction between the somatic myoepithelium and the oocytes within. The somatic gonad contracts only sporadically while the oocyte nearest the spermatheca completes maturation. After maturation is complete, contractions of the myoepithelium increase, and the oocyte is squeezed into the spermatheca for fertilization. This observation suggests either that the mature oocyte signals the myoepithelium to increase contractions or that increased myoepithelium contractions signal the completion of oocyte maturation.

I am grateful to James Lessard (Children's Hospital Research Foundation, Cincinnati, OH) and Jonathan Scholey (University of Colorado at Boulder) for providing antibodies, to Rudi Turner for doing the electron microscopy and providing the micrograph in Fig. 2 *d*, and to L. S. B. Goldstein, William Saxton, Gary Radice, and members of my lab for valuable discussions and critical reading of the manuscript.

This research was supported by a grant to S. Strome from the National Institutes of Health (GM 34059).

Received for publication 10 April 1986, and in revised form 6 August 1986.

References

1. Albertson, D. G. 1984. Formation of the first cleavage spindle in nematode embryos. *Dev. Biol.* 101:61–72.

2. Albertson, D. G. 1985. Mapping muscle protein genes by *in situ* hybridization using biotin-labeled probes. *EMBO (Eur. Mol. Biol. Organ.) J.* 4: 2493–2498.

3. Bond, M., and A. V. Somlyo. 1982. Dense bodies and actin polarity in vertebrate smooth muscle. *J. Cell Biol.* 95:403–413.

4. Boschek, C. B., B. M. Jockusch, R. R. Friis, R. Back, E. Grundman, and H. Bauer. 1981. Early changes in the distribution and organization of microfilament proteins during cell transformation. *Cell.* 24:175–184.

5. Brenner, S. 1974. The genetics of *Caenorhabditis elegans*. *Genetics.* 77:71–94.

6. Buckley, I. K. 1981. Fine structural and related aspects of nonmuscle cell motility. *Cell & Muscle Motil.* 1:135–203.

7. Carley, W. W., L. S. Barak, and W. W. Webb. 1981. F-actin aggregates in transformed cells. *J. Cell Biol.* 90:797–802.

8. Deleted in press.

9. Deppe, U., E. Schierenberg, T. Cole, C. Krieg, D. Schmitt, B. Yoder, and G. von Ehrenstein. 1978. Cell lineages of the embryo of the nematode *Caenorhabditis elegans*. *Proc. Natl. Acad. Sci. USA.* 75:376–380.

10. Drenckhahn, D., U. Groschel-Stewart, J. Kendrick-Jones, and J. M. Scholey. 1983. Antibody to thymus myosin; its immunological characterization and use for immunocytochemical localization of myosin in vertebrate nonmuscle cells. *Eur. J. Cell Biol.* 30:100–111.

11. Edgar, L. G., and J. D. McGhee. 1986. Embryonic expression of a gut-specific esterase in *Caenorhabditis elegans*. *Dev. Biol.* 114:109–118.

12. Ellis, R. A. 1965. Fine structure of the myoepithelium of the eccrine sweat glands of man. *J. Cell Biol.* 27:551–563.

13. Euteneuer, U., and M. Schliwa. 1985. Evidence for the involvement of actin in the positioning and motility of centrosomes. *J. Cell Biol.* 101:96–103.

14. Files, J., S. Carr, and D. Hirsh. 1983. Actin gene family in *Caenorhabditis elegans*. *J. Mol. Biol.* 164:335–375.

15. Flanagan, M. D., and S. Lin. 1980. Cytochalasins block actin filament elongation by binding to high affinity sites associated with F-actin. *J. Biol. Chem.* 255:835–838.

16. Goldman, R. D., B. Chojnacki, and M. J. Yerna. 1979. Ultrastructure of microfilament bundles in baby hamster kidney (BHK-21) cells. *J. Cell Biol.* 80:759–766.

16a. Goldman, R., T. Pollard, and J. Rosenbaum, editors. 1976. Cell motility. *Cold Spring Harbor Conf. Cell Proliferation.* Vol. 3 (Book A):456 pp.

17. Hirsh, D., D. Oppenheim, and M. Klass. 1976. Development of the reproductive system in *Caenorhabditis elegans*. *Dev. Biol.* 49:200–219.

18. Hoch, H. C., and R. C. Staples. 1983. Visualization of actin *in situ* by rhodamine-conjugated phalloidin in the fungus *Uromyces phaseoli*. *Eur. J. Cell Biol.* 32:52–58.

19. Jeffery, W. R., and S. Meier. 1983. A yellow cresent cytoskeletal domain in ascidian eggs and its role in early development. *Dev. Biol.* 96:125–143.

20. Kilmartin, J. V., and A. E. M. Adams. 1984. Structural rearrangements of tubulin and actin during the cell cycle of the yeast Saccharomyces. *J. Cell Biol.* 98:922–933.

21. Kimble, J., and D. Hirsh. 1979. The postembryonic cell lineages of the hermaphrodite and male gonads in *Caenorhabditis elegans*. *Dev. Biol.* 70: 396–417.

22. Landel, C. P., M. Krause, R. H. Waterston, and D. Hirsh. 1984. DNA rearrangements of the actin gene-cluster of *C. elegans* accompany reversion of three muscle mutants. *J. Mol. Biol.* 180:497–513.

23. Langanger, G., M. Moeremas, G. Daneels, A. Sobieszek, M. De Brabandes, and J. De Mey. 1986. The molecular organization of myosin in stress fibers of cultured cells. *J. Cell Biol.* 102:200–209.

24. Laufer, J. S., P. Bazzicalupo, and W. B. Wood. 1980. Segregation of developmental potential in early embryos of *Caenorhabditis elegans*. *Cell.* 19:569–577.

25. Lehtonen, E., and R. A. Badley. 1980. Localization of cytoskeletal proteins in preimplantation mouse embryos. *J. Embryol. Exp. Morphol.* 55: 211–225.

26. Lessard, J. L., S. Scheffter, L. Engel, and K. Tepperman. 1983. Immunofluorescent localization of actins in differentiating chick myoblasts. *J. Cell Biol.* 97 (5, Pt. 2):74a. (Abstr.)

27. MacLean-Fletcher, S., and T. D. Pollard. 1980. Mechanism of action of cytochalasin B on actin. *Cell.* 20:329–341.

28. Maro, B. 1985. Fertilization and the cytoskeleton in the mouse. *BioEssays.* 3:18–21.

29. Maro, B., M. H. Johnson, S. J. Pickering, and G. Flach. 1984. Changes in actin distribution during fertilization of the mouse egg. *J. Embryol. Exp. Morphol.* 81:211–237.

30. Miller, M. R., J. J. Castellot, and A. B. Pardee. 1979. A general method for permeabilizing monolayer and suspension cultured animal cells. *Exp. Cell Res.* 120:421–425.

31. Mollenhauer, H., and D. Morre. 1976. Cytochalasin B but not colchicine inhibits migration of secretory vesicles in root tips of maize. *Protoplasma.* 87:39–48.

32. Nothnagel, E. A., L. S. Barak, J. W. Sanger, and W. W. Webb. 1981. Fluorescence studies on modes of cytochalasin B and phallotoxin action on cytoplasmic streaming in *Chara*. *J. Cell Biol.* 88:364–372.

33. Pollard, T., and R. R. Weihing. 1974. Actin and myosin and cell movement. *CRC Crit. Rev. Biochem.* 2:1–65.

34. Sabatini, D. D., K. Bensch, and R. J. Barnett. 1963. Cytochemistry and electron microscopy: the preservation of cellular ultra-structure and enzymatic activity by aldehyde fixation. *J. Cell Biol.* 17:19–58.

35. Sawada, T., and K. Osanai. 1985. Distribution of actin filaments in fertilized eggs of the ascidian *Ciona intestinalis*. *Dev. Biol.* 111:260–265.

36. Scharf, S. R., and J. C. Gerhardt. 1983. Axis determination in eggs of *Xenopus laevis*; a critical period before cleavage identified by the common effects of cold, pressure, and ultraviolet radiation. *Dev. Biol.* 99:75–88.

37. Schatten, G., and H. Schatten. 1981. Effects of motility inhibitors during sea urchin fertilization. *Exp. Cell Res.* 135:311–330.

38. Schatten, G., C. Simerly, and H. Schatten. 1985. Microtubule configurations during fertilization, mitosis, and early development in the mouse and the requirement for egg microtubule-mediated motility during mammalian fertilization. *Proc. Natl. Acad. Sci. USA.* 82:4152–4156.

39. Schroeder, T. E. 1975. Dynamics of the contractile ring. *In* Molecules and Cell Movement. S. Inoué and R. E. Stephens, editors. Raven Press, New York. 305–334.

40. Schroeder, T. E. 1976. Actin in dividing cells: evidence for its role in cleavage but not mitosis. *Cold Spring Harbor Conf. Cell Proliferation.* Vol. 3 (Book A):265–277.

41. Sheetz, M. P., and J. A. Spudich. 1983. Movement of myosin-coated fluorescent beads on actin cables *in vitro*. *Nature (Lond.).* 303:31–35.

42. Strome, S. 1986. Establishment of asymmetry in early *Caenorhabditis elegans* elbryos: visualization with antibodies to germ cell components. *In* Gametogenesis and the Early Embryo. J. C. Gall, editor. Alan R. Liss, Inc. 77–95.

43. Strome, S., and W. B. Wood. 1982. Immunofluorescence visualization of germline-specific cytoplasmic granules in embryos, larvae, and adults of *Caenorhabditis elegans*. *Proc. Natl. Acad. Sci. USA.* 79:1558–1562.

44. Strome, S., and W. B. Wood. 1983. Generation of asymmetry and segregation of germ-line granules in early *C. elegans* embryos. *Cell.* 35:15–25.

45. Sulston, J. E., E. Schierenberg, J. White, and N. Thomson. 1983. The embryonic cell lineage of the nematode *Caenorhabditis elegans*. *Dev. Biol.* 100:64–119.

46. Tanenbaum, S. W., editor. 1978. Cytochalasins: Biochemical and Biological Aspects. Amsterdam, North Holland. 564 pp.

47. Ward, S., and J. S. Carrel. 1979. Fertilization and sperm competition in the nematode *Caenorhabditis elegans*. *Dev. Biol.* 73:304–321.

48. Warn, R. M., R. Magrath, and S. Webb. 1984. Distribution of F-actin during cleavage of the *Drosophila* syncytial blastoderm. *J. Cell Biol.* 98: 156–162.

49. Waterston, R. H., D. Hirsh, and T. R. Lane. 1984. Dominant mutations affecting muscle structure in *Caenorhabditis elegans* that map near the actin gene cluster. *J. Mol. Biol.* 180:473–496.

50. Waterston, R. H., J. N. Thomson, and S. Brenner. 1980. Mutant with altered muscle structure in *Caenorhabditis elegans*. *Dev. Biol.* 77:271–302.

51. Wieland, T. 1977. Modification of actins by phallotoxins. *Naturwissenschaften.* 64:303–309.

52. Wieland, T., and H. Faulstich. 1978. Amatoxins, phallotoxins, phallolysin, and antamanide: the biologically active components of poisonous Amanita mushrooms. *CRC Crit. Rev. Biochem.* 5:185–260.

53. Wolf, N., J. Priess, and D. Hirsh. 1983. Segregation of germline granules in early embryos of *Caenorhabditis elegans*: an electron microscopic analysis. *J. Embryol. Exp. Morphol.* 73:297–306.

54. Wulf, E., A. Deboben, F. A. Bautz, H. Faulstich, and T. Wieland. 1979. Fluorescent phallotoxin, a tool for the visualization of cellular actin. *Proc. Natl. Acad. Sci. USA.* 76:4498–4503.

55. Zalokar, M. 1974. Effect of colchicine and cytochalasin B on ooplasmic segregation of ascidian eggs. *Wilhelm Roux Arch. Dev. Biol.* 175:243–248.